Ingeniare. Revista Chilena de Ingeniería
ISSN: 0718-3291
facing@uta.cl
Universidad de Tarapacá
Chile

Alvarez-Lugo, Allex E.; Carvajal-Muñoz, Juan S.; Walubita, Lubinda F.
Comparison of the air voids characteristics of different hot mix asphalt (HMA) mixture types
Ingeniare. Revista Chilena de Ingeniería, vol. 22, núm. 1, enero, 2014, pp. 74-87
Universidad de Tarapacá
Arica, Chile

Comparison of the air voids characteristics of different hot mix asphalt (HMA) mixture types

Comparación de las características de los vacíos en diferentes tipos de mezclas asfálticas en caliente

Allex E. Alvarez-Lugo[1] Juan S. Carvajal-Muñoz[1] Lubinda F. Walubita[2]

Recibido 10 de julio de 2012, aceptado 30 de septiembre de 2013
Received: July 10, 2012 Accepted: September 30, 2013

RESUMEN

La estructura interna de las mezclas asfálticas en caliente (MAC) juega un papel importante en la respuesta y desempeño de estas mezclas de pavimentación. El objetivo de este artículo es realizar una comparación cuantitativa de las diferencias de estructura interna –evaluada en términos de las características de sus vacíos– de cuatro tipos de MAC. Aunque la evaluación del desempeño de las MAC analizadas está fuera del alcance del estudio, la comparación realizada es útil como punto de partida para mejorar la comprensión de las diferencias existentes a nivel macroscópico entre varios tipos de MAC. Las características de los vacíos (i.e., contenido, distribución y tamaño) fueron calculadas mediante el análisis de imágenes de especímenes producidos usando el compactador giratorio Superpave (CGS), capturadas empleando tomografía computarizada de rayos X. Los resultados y análisis correspondientes sugirieron que las mezclas estudiadas presentan distribuciones verticales irregulares de contenido total de vacíos y tamaño de vacíos, con grados de heterogeneidad dependientes del tipo de mezcla, pero no del espécimen. En consecuencia, el procedimiento específico usado para obtener especímenes compactados con el CGS debería diseñarse a partir de la altura del espécimen y el tipo de mezcla. Adicionalmente, el análisis comparativo indicó que las mezclas consideradas como "difíciles de compactar" en el laboratorio (i.e., mezclas drenantes fabricadas con asfalto caucho) no exhibieron el grado de heterogeneidad más alto en su estructura interna. Esta conclusión sugiere la necesidad de manejar en forma adecuada todos los tipos de MAC para asegurar la obtención de verdaderos especímenes réplica.

Palabras clave: Mezcla asfáltica en caliente, estructura interna de la mezcla, tomografía computarizada con rayos X, vacíos, pavimentos.

ABSTRACT

The internal structure of the hot mix asphalt (HMA) mixtures plays an important role in the response and performance of these paving mixtures. The objective of this paper is to conduct a quantitative comparison of the differences in internal structure –evaluated in terms of the air voids (AV) characteristics– of four HMA mixture types. Although the performance assessment of the HMA mixtures analyzed is out of the scope of this paper, the comparison conducted is useful to improve the understanding of the differences exhibited, at the macroscopic level, by different HMA mixture types. The AV characteristics (i.e., content, distribution, and size) were computed based on analysis of X-ray Computed Tomography images obtained from specimens compacted using the Superpave gyratory compactor (SGC). Corresponding results and analysis suggested that the mixtures studied presented irregular vertical distributions of total AV content and AV size, with a degree of heterogeneity that is mixture dependent, but not specimen

[1] Departamento de Ingeniería Civil. Universidad del Magdalena. Santa Marta, Magdalena, Colombia. Código postal: 470004. E-mail: allexalvarez@yahoo.com; ing.juancarvajal@yahoo.com
[2] Texas A&M Transportation Institute - The Texas A&M University System. College Station, Texas, United States. Código postal: 77840. E-mail: lfwalubita@hotmail.com

dependent. Consequently, the specific laboratory procedure used to obtain SGC compacted specimens should be designed based on both the specimen height and mixture type. In addition, the comparative analysis also indicated that the mixtures considered as "difficult to handle" in the laboratory (i.e., PFC mixtures fabricated with asphalt rubber) did not exhibit the highest degree of heterogeneity in their internal structure. This conclusion suggests the need for proper handling of all types of HMA mixtures to get true replicate specimens.

Keywords: Hot mix asphalt (HMA) mixture, mixture internal structure, X-ray computed tomography (X ray CT), air voids, pavements.

INTRODUCTION

The internal structure of hot mix asphalt (HMA) mixtures is related to their response and performance [1-3]. This internal structure can be characterized in terms of the aggregate structure (i.e., contact, orientation, and distribution) and air voids (AV) characteristics (i.e., size, distribution, and connectivity) [4]. Thus, previous research computed the internal structure of some dense-graded HMA mixtures [3, 5-11], stone matrix asphalt (SMA) [10], and open-graded HMA mixtures (i.e., permeable friction course (PFC) or new generation open-graded friction course (OGFC)) [10; 12] for diverse specific applications and analyses. However, a systematic analysis and comparison of the mixture internal structure of different HMA types (i.e., differentiated by the aggregate gradation) is still required to better understand their internal structure differences and possible effects on the mixture response and performance.

Consequently, the main objective of this research study is to establish a comparison–describe numerical differences–between the internal structures of a diverse array of laboratory-compacted HMA mixtures. This comparison is useful to enhance the understanding of the differences in performance exhibited, at the macroscopic level, by different HMA mixture types. Within the scope of this paper, the comparison is set in terms of the analysis of the *vertical distribution* of AV content and AV size of both dense-graded and open-graded mixtures.

In particular, the analysis carried out for comparing the vertical distributions included determination of the: (*i*) cumulative frequencies for the total AV content and AV size and (*ii*) heterogeneity indices of the total AV content.

The comparison of the internal structure conducted in this research included three types of dense-graded HMA mixtures–Type B, Type C, and Type D as per Texas specifications [13]–and two types of PFC mixtures fabricated using asphalt rubber (AR-PFC) and polymer modified asphalts (PM-PFC). These PFC mixtures differed in their gradation to be designed at the same target total AV content (i.e., 20±2%) with different asphalt cement binder (or asphalt) contents. The parameters associated with the HMA mixture internal structure were computed based on non-destructive X-ray Computed Tomography (X-ray CT) and subsequent application of image analysis techniques on specimens compacted using the Superpave gyratory compactor (SGC).

In the paper, after this introductory section, a description of the mixtures analyzed is presented, followed by the methods and materials and a brief description of the methodology conducted for X-ray CT and image analysis. Then, the results and discussion are presented in terms of the main outcomes. A section of conclusions and recommendations is then provided to complete the paper.

DESCRIPTION OF THE MIXTURES ANALYZED

Dense-graded HMA mixtures are composed of asphalt and a well or continuously graded aggregate. Conventional HMA consists of mixtures with a nominal maximum aggregate size (NMAS) in the range of 12.5 mm to 19 mm. This material makes up the bulk of HMA used in the United States [14]. There are two other categories included for this type of asphalt mixtures: (*i*) large stone mixtures and (*ii*) sand asphalt. The former is mainly composed of coarse aggregate with a nominal maximum size of approximately 25 mm. The second, also

termed sheet asphalt, is composed of aggregate particles that pass the 9.5-mm sieve. Typically, the rut resistance of this material is fair to low, unless appropriate materials are used for its production (i.e., manufactured sand or rough-textured natural sand). Any of these types of HMA require different processes for plant production and the wears may vary from one to another, as a result of the sizes and the physical properties of each material.

In Texas, Type B mixtures–typically coarse-graded 22-mm NMAS mixtures–are used as intermediate layers within the HMA pavement structures [15]. Their primary function is often load dissipation as well as providing rut resistance to the overall pavement structure due to their coarse aggregate gradation. These mixtures are often used on high-traffic volume roads with a high proportion of trucks.

The dense-graded Type C and D mixtures are typically used as surface mixtures or overlays, usually ranging from 9.5- to 19-mm in NMAS [15].

PFC mixtures are a special type of HMA composed of a high quality aggregate that allows obtaining a coarse granular skeleton that develops stone-on-stone contact and high connectivity between the AV in the mixture. The contact between coarse aggregates is responsible for the mixture resistance to disintegration and permanent deformation. The fine aggregates partially fill the spaces of the AV created by the coarse granular skeleton in the compacted PFC mixture. In addition, the high total and connected AV content is related to the high PFC permeability (as compared to that of conventional dense-graded HMA mixtures), as well as their noise reduction capacity [16].

MATERIALS AND METHODS

Table 1 summarizes the main characteristics of the HMA mixtures evaluated. These mixtures were designed in accordance with the Texas Department of Transportation (TxDOT) mix design procedures for dense-graded HMA and PFC mixtures [17] and corresponding material specifications [13]. Table 2 shows the aggregate gradations for the HMA mixtures characterized.

All the HMA specimens were compacted in the laboratory using a Servopac SGC and in accordance with the test method Tex-241-F [17] to produce 152.4 mm in diameter specimens at three heights (i.e., 62.5 ± 2 mm, 115 ± 5 mm, and 150 ± 5 mm). The shortest specimens are typically compacted for subsequent evaluation of resistance to permanent deformation using the Hamburg wheel tracking test and/or evaluation of HMA indirect tensile strength, fracture parameters, etc [18]. The 115 mm in height specimens are typically used for both mix design and mixture performance evaluation and the tallest specimens (≥ 150 mm) are used for evaluation of HMA mixture response parameters including modulus, flow number, flow time, permanent deformation, thermal coefficient, HMA direct tensile strength, fracture parameters, etc (after cutting and coring to 100 mm in diameter) [15].

After compaction, the specimen testing process included evaluation of total AV content in the

Table 1. Characteristics of the HMA mixtures.

Mixture type	Asphalt type	Aggregate type	OAC (%)	NR
Type B	PG 64-22	Limestone	4.3	2
Type C	PG 76-22	Crushed gravel	5.3	2
Type D-Atlanta or D-AT	PG 64-22	Quartzite + 20% RAP	5.1	3
Type D-Chico or D-CH	PG 70-22	Limestone	5.0	2
1-PM-PFC	PG-76-22	Sandstone, Limestone	6.1	2
2-PM-PFC	PG-76-22	Sandstone	6.6	2
3-PM-PFC	PG-76-22	Limestone	6.5	2
4-PM-PFC	PG-76-22	Limestone	6.4	2
5-PM-PFC	PG-76-22	Granite, Limestone	5.9	2
6-PM-PFC	PG-76-22	Limestone	5.8	2
1-AR-PFC	Type II AR, GB (AC-10+16% CR)	Sandstone, Limestone	8.1	2
2-AR-PFC	Type II AR, GB (AC-10+17% CR)	Granite, Limestone	8.0	2
3-AR-PFC	Type II AR, GB (AC-10+17% CR)	Sandstone	8.3	2

OAC = optimum asphalt content (%); NR = number of replicates; PM = polymer modified; AR = asphalt rubber; CR = crumb rubber; GB = grade B (rubber gradation [13]), RAP=reclaimed asphalt pavement.

Table 2. Aggregate gradations.

Sieve	Dense-graded HMA mixtures				PM-PFC mixtures						AR-PFC mixtures		
	B	C	D-AT	D-CH	1-PM	2-PM	3-PM	4-PM	5-PM	6-PM	1-AR	2-AR	3-AR
19 mm	100	100	100	100	100	100	100	100	100	100	100	100	100
12.5 mm	97.3	94.6	99	100	90.3	81	85.3	90.5	80.2	84.5	99	95.6	99.7
9.5 mm	76.9	82.0	91.8	99.2	59.5	43	59.4	50.9	57.7	52.8	54.6	54.9	75.7
#4	44.6	52.5	56.5	63.8	10.1	15.5	18.6	3.2	15.9	6.6	5	4	7.9
#8	32.9	31.0	37.6	38.2	5.2	6.7	2.0	1.5	6.0	4.2	1.9	2.1	1.1
#200	2.1	2.6	5.9	3.3	2.3	2.2	1.6	1.1	2.1	2.4	1.0	0.8	0.6

laboratory and X-ray CT scanning. The total AV content for dense-graded HMA was evaluated by the traditional water displacement method [15], while PFC mixtures were assessed using dimensional analysis–assuming the specimen as a regular cylinder for computing the total volume–as suggested in previous research [19-20]. Details on the X-ray CT and subsequent image analysis are provided in the next section.

X-Ray CT image processing and indices for analysis of the mixture internal structure

For each laboratory specimen, X-ray CT scanning allowed obtaining grayscale images (i.e., with a range of 256 colors, from 0-black to 255-white) 1-mm apart (i.e., transversal parallel sections along the specimen height with approximate resolution of 0.17 mm/pixel). This is a non-destructive procedure that permits the subsequent evaluation of the internal structure of HMA mixtures based on the density differences in the constituent materials. Details on the X-ray CT principles of operation are reported elsewhere [21-22].

Computation of the internal structure for each specimen of the different HMA mixtures analyzed included determination of the *vertical distribution* of both total AV content and AV size (i.e., mean radius of AV). For each specimen, these computations were based on the analysis of the group of grayscale images representing a particular specimen. This image analysis was conducted as described in detail in previous research [20, 23], and it is subsequently summarized.

The first stage of image analysis allowed cropping the raw grayscale images to eliminate the external voided area that existed in the images produced by the X-ray CT scanner. This process was performed by using the software *ImageJ 1.41o* [24]. The second stage of image analysis, performed on the cropped grayscale images, allowed discriminating in the output black and white images the solid phase (white) and void phase–AV corresponding to the total AV content–(black) in each image of the specimen. The last stage of image analysis was conducted on the black and white images to compute the total AV content and AV size per image. This analysis was performed using an image analysis macro [23] developed for the Image-Pro® Plus software [25]. Corresponding computations allowed generating the vertical distribution of both total AV content and AV size.

Equations (1) to (3) were used to compute the total AV content for an individual black and white image (AV_i), the total AV content of a particular specimen (AV_S), and the mean radius of the AV–representing the mean size of AV in image *i*–($\overline{r_i}$):

$$AV_i = \frac{A_{v_i}}{A_T} \ (\%) \tag{1}$$

$$AV_s = \frac{\sum_{i=1}^{N} AV_i}{N} \ (\%) \tag{2}$$

$$\overline{r_i} = \sqrt{\frac{A_{vi}}{\pi M_i}} \ (\text{mm}) \tag{3}$$

where A_{vi} is the area of the AV in image *i*, A_T is the cross-sectional area (circle area) of image *i,* and *N* is the number of images representing a specimen. M_i is the number of AV in image *i*.

The vertical heterogeneity index, $V_{er}H_{index}$, for a particular specimen was used as an index to assess

the heterogeneity of its vertical distribution of total AV content and it was computed as follows:

$$V_{er}H_{index} = \frac{k}{N}\sum (V_i - \overline{V})^2 \quad (4)$$

where k is the number of successive images (i.e., originally 1 mm apart) grouped to compute the index, V_i is the mean total AV content (%) of k successive images, and $\overline{V}$ is the mean total AV content (%) measured for the specimen, which is equal to AV_S (equation (2)). The computation of the vertical heterogeneity index required grouping k images–for different values of k/N–. Additional discussion on this procedure is presented in the results and analysis section.

Previous research [7] quantified the vertical heterogeneity of total AV content values in compacted specimens of a dense-graded HMA (i.e., 12.5 mm Superpave mixture). However, this research [7] did not include evaluation of replicate specimens, the effect of the specimen height and the comparison between HMA mixture types. Thus, this research study attempted to evaluate the vertical heterogeneity index of different HMA mixture types, with varying specimen heights, and replicate specimens to achieve a broader evaluation of the vertical heterogeneity of the total AV content in HMA mixtures.

RESULTS AND ANALYSES

This section presents the results and corresponding discussion on the characterization of HMA mixture internal structure. The results are first presented in terms of the patterns of vertical distribution of both AV content and AV size for replicate SGC compacted specimens. Then, these vertical distributions are further analyzed based on the comparison of the following: (*i*) cumulative frequency distributions of both AV content and AV size, and (*ii*) heterogeneity of the vertical distribution of total AV content, computed in terms of the vertical heterogeneity index. The final section includes a comparison of the vertical distribution of the total AV content in PFC mixtures.

Comparison of vertical distribution of both AV content and AV size for replicate specimens

Figure 1 presents the vertical distribution of the total AV content for the Type C, Type B, Type D, PM-PFC, and AR-PFC mixtures. Each mixture type was evaluated using replicate specimens–identified in the figure by the last digit in the legend–. The data for the Type D-CH mixture is not presented in the figure for clarity reasons. Similarly, although nine PFC mixtures were analyzed, only the data of two of them were included in Figure 1 for illustrative purposes only.

The purpose of this analysis was to establish whether the laboratory methods used to obtain the specimens are appropriate for testing purposes with no representative differences among replicate specimens.

These replicate specimens exhibited differences of less than 3 percentage points along the vertical distribution of total AV content, except for the PFC mixtures, which exhibited differences of up to 6 percentage points. As compared to the target total AV content, these differences could be big enough to differentiate particular sections of the SGC specimens. However, based on hypothesis tests, performed using Statgraphics Centurion XVI.I [26], no differences between the mean values for the total AV content were found between the replicate specimens with a 95% confidence level. Based on this statistical analysis, the SGC specimens analyzed can be considered as true replicate specimens in terms of the AV characteristics computed to quantify their mixture internal structure. This conclusion supports proper reproducibility of the SGC replicate compacted specimens.

In addition, data shown in Figure 1 provide evidence of irregular vertical distributions of the total AV content in the SGC specimens of all the HMA types evaluated. Heterogeneous distributions were reported in previous research for dense-graded HMA specimens produced using the SGC [1, 3-4, 6, 11, 27-28]. In addition, data shown in Figure 2 for the same replicate specimens presented in Figure 1 suggest that the vertical distributions of the AV size (i.e., AV radius) closely resemble the "C" shape shown in Figure 1 for the vertical distribution of the total AV content. The distributions computed for dense-graded HMA mixtures are also consistent with those reported in previous research [6] for this type of mixtures.

As discussed in previous research [7, 27], these irregular vertical distributions are related to the

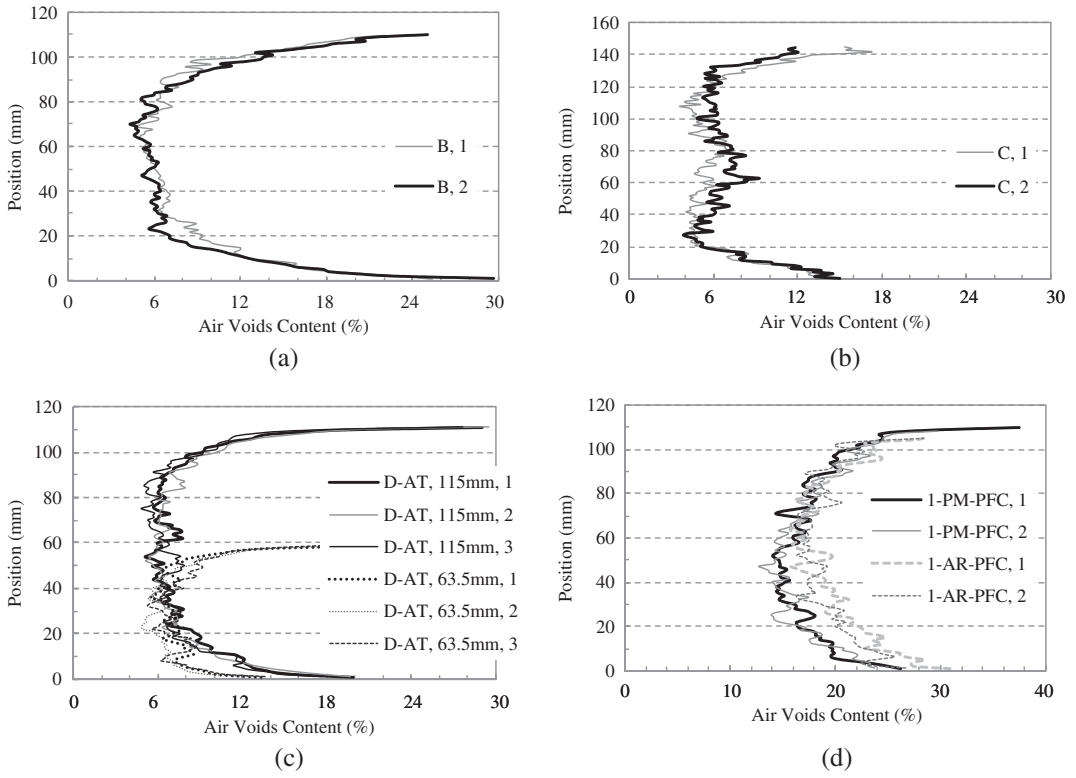

Figure 1. Vertical distribution of total AV content (replicate specimens) for Type B (a), Type C (b), Type D (c), and PFC (d) mixtures.

distribution of compaction energy in the SGC specimens. However, as subsequently discussed, the degree of heterogeneity of each particular vertical distribution is related to the HMA mixture type (i.e., mixture gradation).

Figures 3 and 4 show, respectively, a comparison of the mean vertical distributions of AV content and AV size computed based on the replicate specimens previously discussed in Figures 1 and 2. However, the mean values of the PM-PFC and AR-PFC mixtures were computed, respectively, by including the data for the six PM-PFC and three AR-PFC mixtures analyzed (Table 1). The same approach was applied for all subsequent computations involving the PFC mixtures.

Direct comparison of the mean vertical distributions of AV content and AV size indicates that the specimen height and the mixture type are related to the heterogeneity of these AV characteristics computed for the SGC specimens. For example, comparison of the specimens analyzed from the Type C mixture (145 mm in height), Type D-AT mixture (115 mm in height), and Type D-AT (63.5 mm in height) suggest that the pattern of the vertical distribution of the AV size (Figure 4) can change as a function of the height of the SGC compacted specimen. A similar conclusion can be obtained by comparing the vertical distributions of the total AV content (Figure 3). The heterogeneity of the total AV content distribution for the different types of HMA mixtures is further discussed in the next sections based on both the cumulative frequency distribution and the vertical heterogeneity index of the total AV content.

Comparison of the cumulative frequency distributions of AV content and AV size

The cumulative frequency of the mean total AV content values for the different HMA mixtures analyzed is shown in Figure 5. In addition, Figure 6 shows the cumulative frequency of the mean AV size values for the same HMA mixtures.

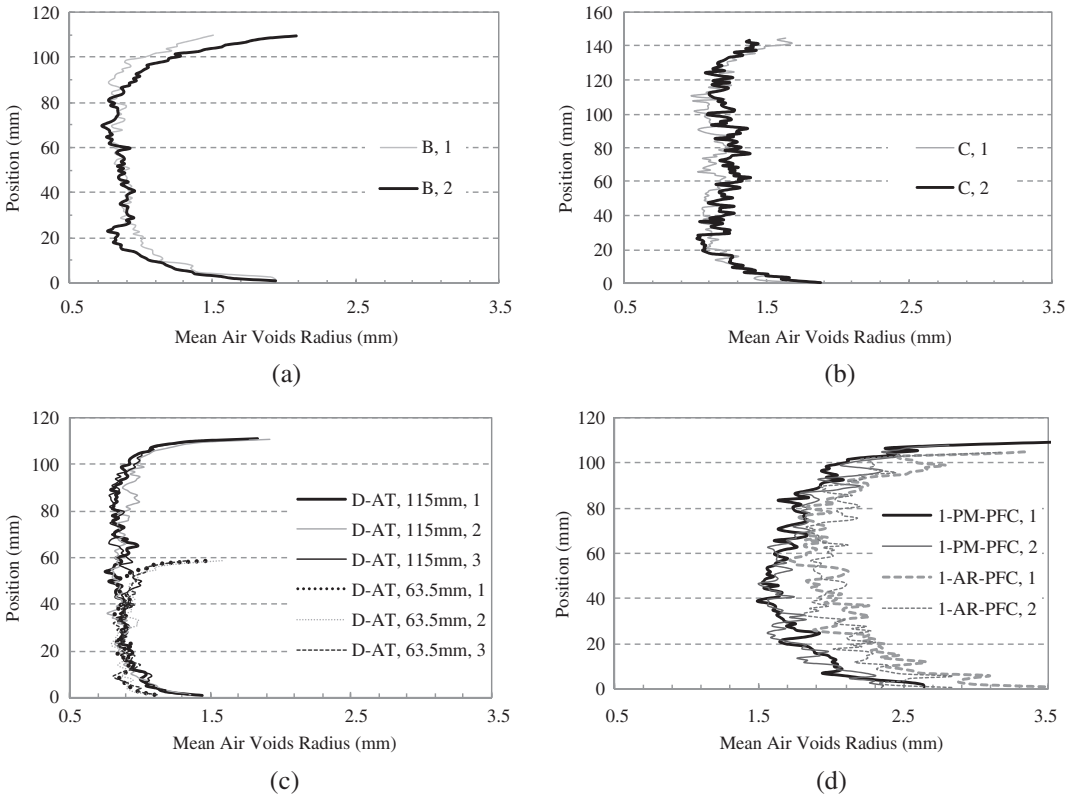

Figure 2. Vertical distribution of the AV size (replicate specimens) for the Type B (a), Type C (b), Type D (c), and PFC (d) mixtures.

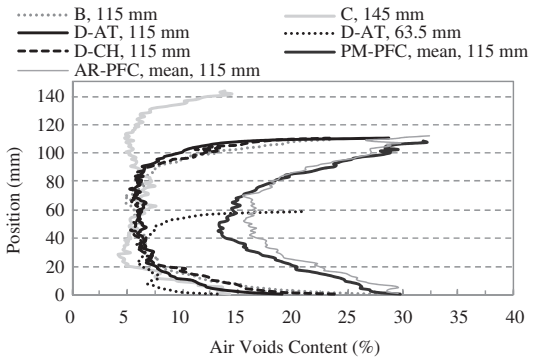

Figure 3. Comparison of mean vertical distribution of total AV content for different HMA mixture types and specimen heights.

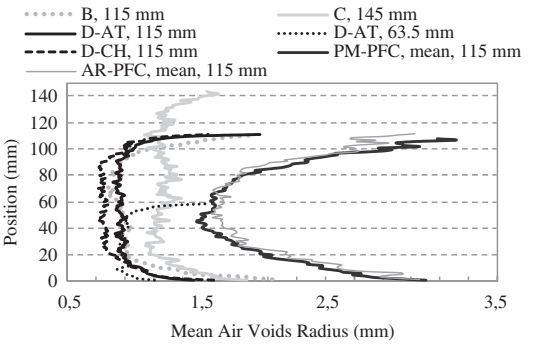

Figure 4. Comparison of mean vertical distribution of AV size for different HMA mixture types and specimen heights.

As expected, corresponding data suggests that the PFC mixtures systematically exhibit larger AV than the dense-graded HMA mixtures. In fact, in terms of the mean values of the AV radius, summarized in the Table 3, the PFC mixtures can exhibit AV twice the size of the AV contained in the dense-graded HMA mixtures.

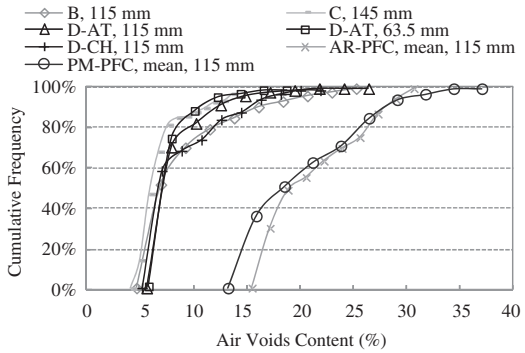

Figure 5. Cumulative frequency of total AV content for different HMA mixtures.

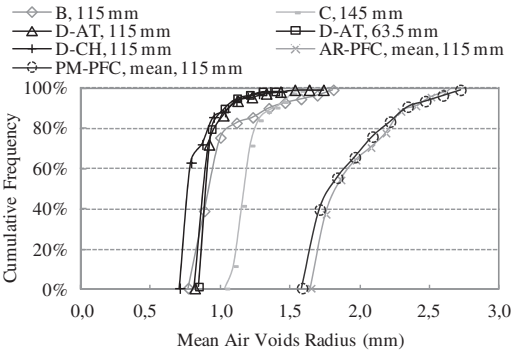

Figure 6. Cumulative frequency of the AV size for different HMA mixtures.

Table 3. Mean values of the total AV content and AV radius and corresponding ranges.

Specimen	TAVC (%)	Range TAVC (%)	AVR (mm)	Range AVR (mm)
B-115 mm	9.0	1.1	1.0	0.1
D-CH-115 mm	8.7	0.7	0.8	0.04
D-AT-115 mm	8.2	0.8	0.9	0.05
D-AT-63.5 mm	7.8	1.1	0.9	0.1
C-145 mm	6.8	0.6	1.2	0.1
1-PM-PFC-115 mm	18.0	1.2	1.9	0.1
2-PM-PFC-115 mm	19.6	1.9	2.2	0.2
3-PM-PFC-115 mm	16.6	1.8	1.6	0.1
4-PM-PFC-115 mm	20.2	2.0	2.0	0.2
5-PM-PFC-115 mm	18.7	1.2	2.0	0.1
6-PM-PFC-115 mm	16.5	1.6	1.7	0.2
1-AR-PFC-115 mm	19.9	1.8	2.2	0.2
2-AR-PFC-115 mm	19.9	1.2	1.9	0.1
3-AR-PFC-115 mm	18.2	2.5	2.3	0.2

TAVC= total air voids content; AVR=air voids radius.

Comparison of the dense-graded HMA mixtures compacted to 115 mm, based on the data presented in both Figure 6 and Table 3, suggests that the Type B mixture exhibits the largest AV, which is theoretically expected given that this mixture has the coarsest aggregate gradation of all the mixtures compared. However, these dense-graded mixtures exhibited minimum differences in the cumulative frequency distribution of the total AV content (Figure 5). These results suggest that the indicated differences in the AV size can be related not only to the aggregate gradation, but to the structure obtained by the aggregate skeleton configuration in the dense-graded HMA mixtures. In turn, this configuration can vary depending on several factors that include the gradation and geometrical characteristics of the aggregate, asphalt properties related to the mixture workability, and the distribution of the compaction energy.

The distribution of energy in the SGC–related to the height of the compacted specimens [7]–has an effect on the internal structure of the HMA mixtures as shown by the Type C mixture specimen compacted to 145 mm. Although this specimen has the lowest total AV content of all the dense-graded HMA mixtures (at 6.8 %; Table 3), it contains the largest AV of all these mixtures (Figure 6), suggesting that a different aggregate structure could be obtained in the tallest specimen as compared to that of the dense-graded HMA specimens compacted to 115 mm in height.

Comparison of the vertical heterogeneity index of total AV content

Figure 7 shows a comparison of the vertical distribution of the total AV content, for subsequent computation of the vertical heterogeneity index, without grouping the images (i.e., original data from X-ray CT images taken each 1 mm) and after grouping the images for a *k/N* value of 3.8%; i.e., grouping 4 successive images (see equation (4)) in PFC mixtures.

As shown in Figure 8, the selection of the *k/N* value–defining the vertical distribution of the total AV content as exemplified in Figure 7–modifies the magnitude of the vertical heterogeneity index as computed based on equation (4). The index values shown in Figure 8 correspond to mean values computed based on the replicate specimens studied. Smaller values of the vertical heterogeneity index

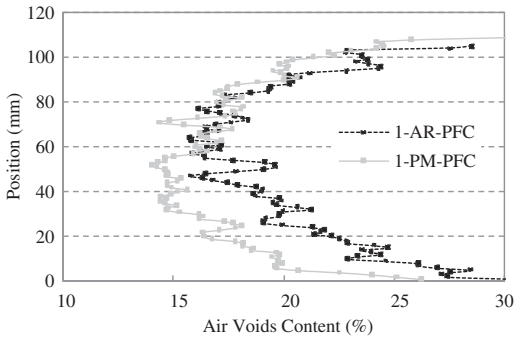

(a)

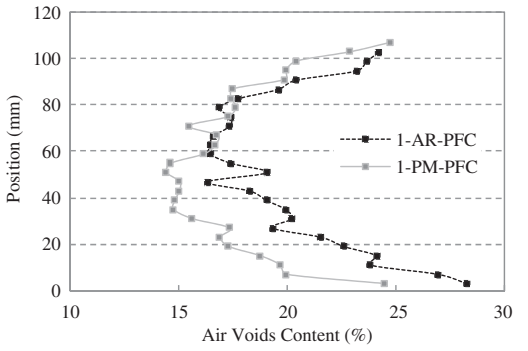

(b)

Figure 7. Vertical distribution of the total AV content before grouping (a) and after grouping images with a selected *k/N* value (b).

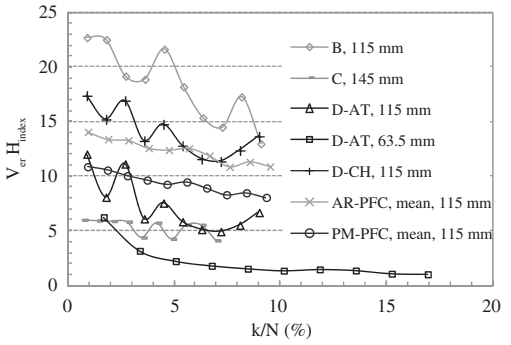

Figure 8. Mean vertical heterogeneity index values for different HMA mixtures.

are indicative of a more homogeneous vertical distribution of the total AV content.

Data presented in Figure 8 suggests that the selection of the *k/N* value, for subsequent computation of the vertical heterogeneity index, is mixture dependent. In some cases (e.g., Type C and AR-PFC mixtures) the index tends to exhibit a steady value as the *k/N* value increases. However, for the same range of *k/N* values used to analyze the Type C and the AR-PFC mixtures, the Type B and Type D mixtures showed substantial changes in the vertical heterogeneity index values.

Additional computations–not shown in Figure 8 for simplicity of the information presented–suggested that each replicate specimen showed similar tendencies as those shown in Figure 8 in terms of the mean values. This conclusion is expected based on the results of the statistical analysis conducted to evaluate the variability of the vertical distribution of the total AV content values of the replicate specimens included in Figure 1.

The analysis presented based on Figures 1, 2, and 8 provide evidence of the heterogeneity in the vertical distribution of the total AV content in the SGC specimens of all the HMA mixtures analyzed. As proposed in previous research conducted on PFC mixtures [29] and dense-graded HMA mixtures [7], a simple way to reduce the heterogeneity of the vertical distribution of the AV is by cutting the extreme sections of the specimens. Figure 9 shows the vertical heterogeneity index values computed for the specimens analyzed after "cutting", for example, 20 mm at their top- and bottom-sections through exclusion of the corresponding scanned images (i.e., electronically cut, or e-cut).

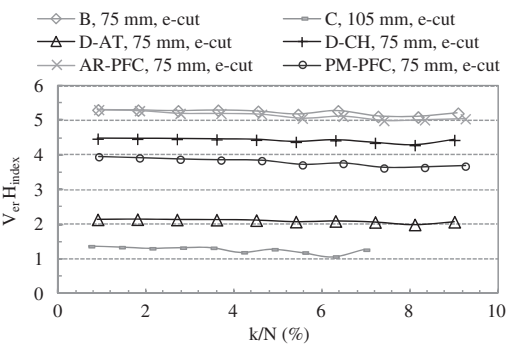

Figure 9. Vertical heterogeneity index values for the e-cut specimens.

Comparison of the vertical heterogeneity index values shown in Figures 8 and 9 indicate a substantial reduction in the heterogeneity of the vertical distribution of the AV content after cutting the top- and bottom-section of the specimens for all the HMA

mixtures analyzed. In addition, steady values of the index, as a function of the *k/N* values, were obtained. Since the type of specimens to produce for subsequent applications of HMA mixture characterization should be similar to those analyzed in Figure 9, additional analysis for recommendation of an "optimum *k/N* value per mixture" for computation of the index was not pursued.

In addition, the differences in the index values presented in Figure 9 indicate that the "homogeneous e-cut specimens" of the different HMA mixture types exhibit diverse degrees of heterogeneity in the vertical distribution of the total AV content. In order of decreasing heterogeneity, the mixtures analyzed can be ranked as Type B, AR-PFC, Type D-CH, PM-PFC, Type D-AT, and Type C.

The PFC mixtures, and specially the AR-PFC mixtures, are usually considered "difficult to handle" in the laboratory, which may contribute to increase the variability in the SGC compacted specimens due, for example, to aggregate and temperature segregation. However, the PFC mixtures did not report the highest values of the vertical heterogeneity index (Figures 8 and 9). These results suggest the need for proper handling of all mixture types, independently of the apparent macroscopic workability that they can exhibit, to ensure the minimum possible variability in the internal structure of the SGC compacted specimens and in subsequent evaluations of performance and response.

In addition, Figure 10 presents a specific comparison of the vertical heterogeneity index of specimens originally compacted in the SGC at different heights and those electronically cut. The height of the portions that were electronically cut was variable to get specimens of 115 and 63 mm in height. The index was computed by using the *k/N* values indicated in Figure 10. These values correspond to the *k/N* associated with the zone of steady values of the index that can be identified in Figure 8 for the Type D-AT and Type C mixtures.

Corresponding results substantiate that production of shorter specimens, achieved by cutting the 115 mm specimens can lead to more homogeneous specimens (i.e., 63 mm, e-cut specimen; $V_{er}H_{index}$ = 0.87) as compared to those directly compacted in the SGC to 63 mm in height ($V_{er}H_{index}$ = 1.66). The

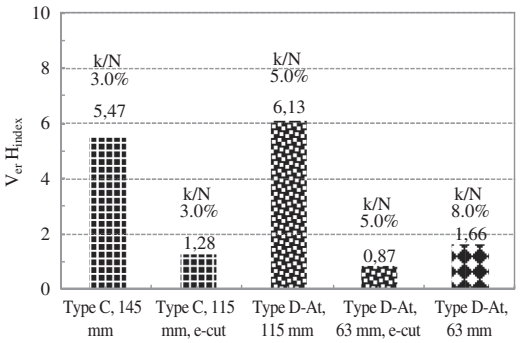

Figure 10. Vertical heterogeneity index values for the SGC specimens of different heights.

same conclusion is valid for production of 115 mm in height specimens based on cutting the specimens compacted in the SGC to 145 mm in height.

Comparison of the vertical distribution of total AV content in PFC mixtures

Figures 11 and 12 show the cumulative frequency distribution of the total AV content and AV size, respectively, for the PFC mixtures. These results suggest that as compared to the PM-PFC mixtures, the AR-PFC mixtures tend to exhibit higher total AV content and AV size values. However, the range of the total AV content and AV size values related to both types of mixture is similar, which suggests that they are comparable.

Figure 13 shows the results of the vertical heterogeneity index values computed for both PM-PFC and AR-PFC mixtures based on different *k/N* values. Corresponding results suggest that for practical purposes, grouping 4 images (i.e., *k=4*;

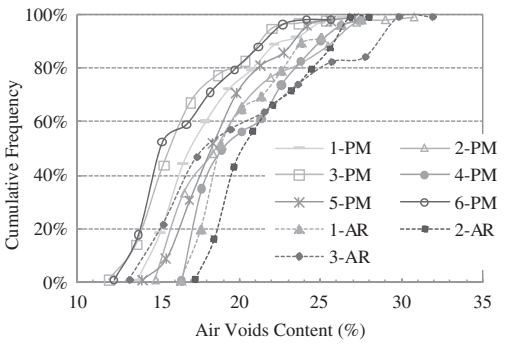

Figure 11. Cumulative frequency of the total AV content for different PFC mixtures.

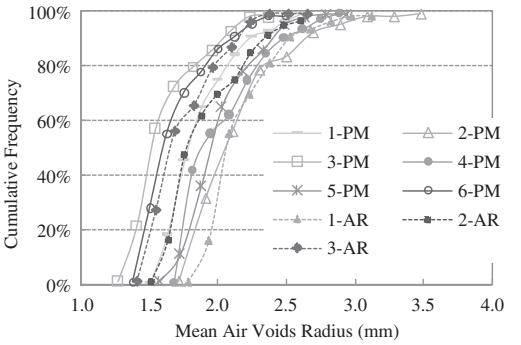

Figure 12. Cumulative frequency of the AV size for different PFC mixtures.

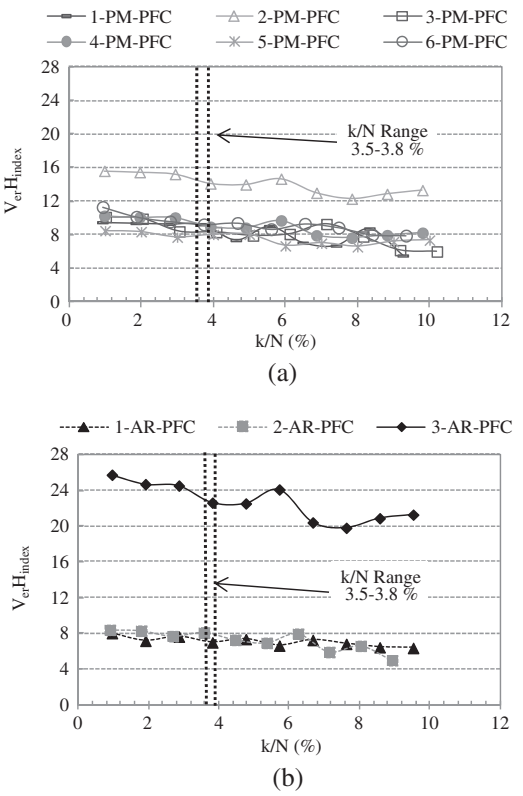

Figure 13. Vertical heterogeneity index values versus *k/N* values for (a) PM-PFC and (b) AR-PFC.

Equation 4) can lead to representative values of the vertical heterogeneity index. For the specimens analyzed, this grouping lead to *k/N* values in the range shown in Figure 13. Therefore, *k=4* can be adapted as a seed value for future evaluation of the heterogeneity of the total AV content in PFC mixtures.

In addition, the differences in the values of the vertical heterogeneity index computed for the PM-PFC and AR-PFC mixtures further support the existence of discrepancies in the internal structure of these two types of PFC mixtures as previously discussed based on Figures 11 and 12.

Figure 14 shows the vertical heterogeneity index values computed for the six PM-PFC mixtures and three AR-PFC mixtures listed in Table 1. Corresponding results provide evidence of variability in the degree of heterogeneity computed for each group (i.e., PM-PFC and AR-PFC) of mixtures fabricated using similar specifications. Since these HMA mixtures were fabricated under the same compaction pattern (i.e., specimen size, temperature, energy, and compactor) in the laboratory, the referred to discrepancies are attributed to differences in the material workability related to the aggregate gradation and geometrical characteristics, asphalt content, and asphalt viscosity.

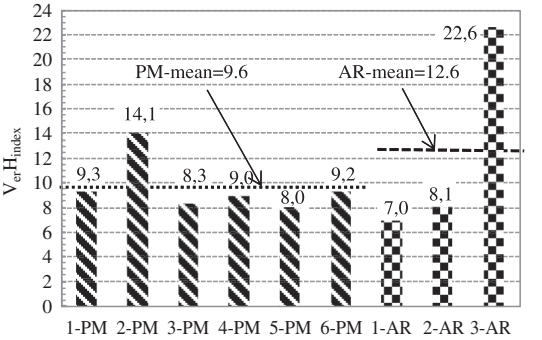

Figure 14. Vertical heterogeneity index values for PM-PFC and AR-PFC mixtures.

In addition, given the variability of the data shown in Figure 14, comparison of the vertical heterogeneity index values of PM-PFC and AR-PFC mixtures does not allow a specific conclusion on which type of PFC mixture exhibits higher variability in the vertical distribution of the total AV content. However, the comparison of the mean values of the vertical heterogeneity index suggests that the PM-PFC mixtures can exhibit a less variable internal structure as compared to that of the AR-PFC mixtures.

These results can partially support the theoretical idea that the higher difficulty experienced in the laboratory for production of replicate specimens of AR-PFC mixtures, as compared to those of PM-PFC

mixtures, is associated with higher variability in the internal structure of the AR-PFC mixtures. This conclusion also motivates the need for proper handling for both types of PFC mixtures to ensure the production of truly replicate specimens–based not only on ensuring similar total AV content values, but to get similar characteristics of the AV structure–.

CONCLUSIONS AND RECOMMENDATIONS

This paper presented a comparison of the internal structure of different types of HMA mixtures, which was evaluated in terms of the AV characteristics. Correspondingly, specimens compacted using the SGC were characterized using X-ray CT scanning and subsequent image analysis. The key findings and conclusions are bullet-listed as follows:

- The comparison of internal structure (i.e., AV characteristics) provided quantitative evidence of the differences in the microstructure of the different types of HMA mixtures analyzed. This information can be useful to enhance the understanding of the differences in behavioral response and performance exhibited, at the macroscopic level, by different types of HMA mixtures.
- The particular procedure used to obtain laboratory specimens based on compaction using the SGC is an aspect that can still be improved. In the future, the specific laboratory procedure used to obtain SGC compacted specimens should be established based on both the mixture type and specimen height targeted for subsequent mixture testing.
- The vertical heterogeneity index values computed suggest that the heterogeneity of the AV characteristics is mixture dependent–and not specimen dependent–. In addition, mixtures considered as "difficult to handle" in the laboratory (i.e., AR-PFC mixtures) did not exhibit the theoretically expected highest degree of heterogeneity (i.e., highest values of the vertical heterogeneity index). These results suggest the need for proper handling of all HMA mixture types, independently of the apparent macroscopic workability that they can exhibit, to ensure the minimum possible variability in the internal structure of the SGC compacted specimens.
- Additional HMA mixtures, which include different types of aggregate, aggregate gradations, asphalt contents, and asphalt types, as well as diverse compaction efforts, should be analyzed in future research to further supplement and validate the findings reported in this study.
- HMA mixture performance was beyond the scope of this study. However, future research focused on the evaluation of the possible correlations between the internal structure of HMA mixtures and performance should be addressed. This evaluation can lead to a better understanding on the dynamics and microscopic processes influencing the macroscopic properties and response of HMA mixtures.

DISCLAIMER

The contents of this paper reflect the views of the authors who are responsible for the facts and accuracy of the data presented herein and do not necessarily reflect the official views or policies of any agency or institute. This paper does not constitute a standard, specification, nor is it intended for design, construction, bidding, contracting, or permit purposes. Trade names were used solely for information and not for product endorsement.

ACKNOWLEDGEMENTS

Special thanks are due to Dr. Amy Epps Martin (Texas A&M University) for the support provided to complete part of the X-ray CT scanning required. Acknowledgments are also due to Dr. Edith Arámbula (Texas A&M University) for facilitating part of the X-ray CT images used in this research. The first and second authors truly thank the support provided by Universidad del Magdalena for this research study.

REFERENCES

[1] G.R. Chehab, E. O'Quinn and R.Y. Kim. "Specimen Geometry Study for Direct Tension Test Based on Mechanical Tests and Air Void Variation in Asphalt Concrete Specimens Compacted by Superpave Gyratory Compactor". Transportation Research Record. Vol. 1723, pp. 125-132. 2000.

[2] Z. Qi Yue, W. Bekking and I. Morin. "Application of Digital Image Processing to Quantitative Study of Asphalt Concrete Microstruture". Transportation Research Record. Vol. 1492, pp. 53-60. 1995.

[3] L. Tashman, E. Masad, J. D'Angelo, J. Bukowski and T. Harman. "X-ray Tomography to Characterize Air Void Distribution in Superpave Gyratory Compacted Specimens". The International Journal of Pavement Engineering. Vol. 3, pp. 19-28. 2002.

[4] E. Masad, B. Muhunthan, N. Shashidhar and T. Harman. "Quantifying Laboratory Compaction Effects on the Internal Structure of Asphalt Concrete". Transportation Research Record. Vol. 1681, pp. 179-185. 1999.

[5] E. Masad, V.K. Jandhyala, N. Dasgupta, N. Somadevan and N. Shashidhar. "Characterization of Air Void Distribution in Asphalt Mixes Using X-ray Computed Tomography". Journal of Materials in Civil Engineering. Vol. 14, pp. 122-129. 2002.

[6] E. Masad, E. Kassem and A. Chowdhury. "Application of Imaging Technology to Improve the Laboratory and Field Compaction of HMA". Report No FHWA/TX-09/0-5261-1. Texas Transportation Institute-Texas A&M University. pp. College Station, TX. 2009.

[7] S. Thyagarajan, L. Tashman, E. Masad and F. Bayomy. "The Heterogeneity and Mechanical Response of Hot Mix Asphalt Laboratory Specimens". International Journal of Pavement Engineering. Vol. 11, pp. 107-121. 2010.

[8] A.E. Alvarez, N. Macias and L.G. Fuentes. "Analysis of Connected Air Voids in Warm Mix Asphalt". DYNA. Vol. 172, pp. 29-37. 2012.

[9] L. Tashman and B. Pearson. "Characterisation of Stone Matrix Asphalt Mixtures". International Journal of Pavement Engineering. Vol. 13, pp. 297-309. 2012.

[10] AASHTO. "Standard Specifications for Transportation Materials and Methods of Sampling and Testing". 27th Edition. Standard T 283-07: Resistance of Compacted Hot Mix Asphalt (HMA) to Moisture-Induced, Washington D.C. T 283-1-T 283-8, 2007.

[11] L. Tashman, E. Masad, B. Peterson and H. Saleh. "Internal Structure Analysis of Asphalt Mixes to Improve the Simulation of Superpave Gyratory Compaction to Field Conditions". Asphalt Pavement Technology. Vol. 70, pp. 605-645. 2001.

[12] A.E. Alvarez, A. Epps Martin and C. Estakhri. "Internal Structure of Compacted Permeable Friction Course Mixtures". Construction and Building Materials. Vol. 24, pp. 1027-1035. 2010.

[13] TxDOT. "Standard Specifications for Construction and Maintenance of Highways, Streets, and Bridges". Austin, TX. 2004.

[14] US Army Corps of Engineers. "Hot Mix Asphalt Paving Handbook". Part I: Project, Organization, Mix Design and Quality Control. 2000.

[15] L.F. Walubita, V. Umashankar, X. Hu, B. Jamison, F. Zhou, T. Scullion, A. Epps Martin and S. Dessouky. "New Generation Mix-Designs: Laboratory Testing and Construction of the APT Test Sections". Report 0-6132-1. Texas Transportation Institute-Texas A&M University. College Station, TX. 2010.

[16] L.A. Cooley Jr., J.W. Brumfield, R.B. Mallick, W.S. Mogawer, M. Partl, L.D. Poulikakos and G. Hicks. "Construction and Maintenance Practices for Permeable Friction Courses". NCHRP Report 640. Washington, D.C. 2009.

[17] TxDOT. "200-F, Bituminous Test Procedures Manual". 2011. Date of visit: October, 2011. URL: http://www.txdot.gov/business/contractors_consultants/test_procedures/tms_series.htm?series=200-F

[18] F. Zhou, S. Hu and T. Scullion. "Integrated Asphalt (Overlay) Mixture Design, Balancing Rutting and Cracking Requirements". Report Nº FHWA/TX-06/0-5123-1. Texas Transportation Institute-Texas A&M University. College Station, TX. 2006.

[19] Ministerio de Obras Públicas y Urbanismo-España. "Mezclas Bituminosas Porosas-MOPU". Madrid, España. 1987.

[20] A.E. Alvarez, A. Epps Martin and C. Estakhri. "Connected Air Voids Content in Permeable Friction Course Mixtures". Journal of Testing and Evaluation. Vol. 37, pp. 254-263. 2009.

[21] N. Shashidhar. "X-ray Tomography of Asphalt Concrete". Transportation Research Record. Vol. 1681, pp. 186-192. 1999.

[22] A. Hassan. "Microstructural Characterisation of Rubber Modified Asphalt Mixtures".

Doctoral Thesis. University of Nottingham. 2012.

[23] E. Masad, E. Arambula, R.A. Ketcham, A.R. Abbas and A.E. Martin. "Nondestructive Measurements of Moisture Transport in Asphalt Mixtures". Journal of the Association of Asphalt Paving Technologists (AAPT). Vol. 76, pp. 919-952. 2007.

[24] W. Rasband. "ImageJ 1.41o". National Institutes of Health.

[25] L.P. Media Cybernetics. "Image-Pro® Plus, Version 5.1.2". Georgia, M.D. 1999.

[26] StatPoint Inc. "Statgraphics Centurion XVI. Versión 16.1.03 (32-bits)". 1998.

[27] A. Partl, A. Flisch and M. Jönsson. "Gyratory Compaction Analysis with Computer Tomography". International Journal of Road Materials and Pavement Design. Vol. 4, pp. 401-422. 2003.

[28] E. Masad, B. Muhunthan, N. Shashidhar and T. Harman. "Internal Structure Characterization of Asphalt Concrete Using Image Analysis". Journal of Computing in Civil Engineering. Vol. 13, pp. 88-95. 1999.

[29] A.E. Alvarez, E.M. Fernandez, A. Epps Martin, O.J. Reyes, L.F. Walubita and G.S. Simate. "Comparison of Permeable Friction Course Mixtures Fabricated Using Asphalt Rubber and Performance-Grade Asphalt Binders". Construction and Building Materials. Vol. 28, pp. 427-436. 2012.